UAS Thermal Infrared Data for Evapotranspiration Estimations with Sugar Beet

Jordan Bates[1], Francois Jonard[1,2], Harry Vereecken[1], Carsten Montzka[1]
1. Institute of Bio- and Geosciences (IBG-3) Forschungszentrum Jülich
2. Earth Observation and Ecosystem Modelling Laboratory, SPHERES Research Unit, Université de Liège

Motivation and Aim

Evapotranspiration (ET) is important for understanding water use and demand. More complete and frequent depictions of ET would allow for improved precision and responsive irrigation planning furthering the farmer's resource efficiency. Unmanned aircraft systems (UAS) offer the ability to collect data at unprecedented spatial resolutions while also allowing on-demand collection for flexibilities in temporal resolutions. More traditional means of ET estimations are performed with lysimeters and flux towers, but these methods only provide limited coverage of the area with limited to no information on the true range and variability, leaving much to be assumed. Satellite remote sensing provides feasible regional scale estimations but can still be considered coarse in cases of smaller scales. Additionally, satellites can only provide data on a fixed schedule which is further complicated with cloud coverage. The greater possibilities in spatial and temporal resolution make UAS the ideal means for ET estimations at scales in the field level and smaller. Most ET models being used with UAS data are those that were created around satellite remote sensing including the two source energy balance (TSEB) model that is used in this study. The experiment included a 10 hectare sugar beet field which has little canopy coverage at the beginning of the growing season to practically complete convergence in the later stages. This allowed for testing of the TSEB model robustness in a dynamic canopy.

Figure 1. Example of the canopy to soil ratio changes as the growing season progresses

Equipment

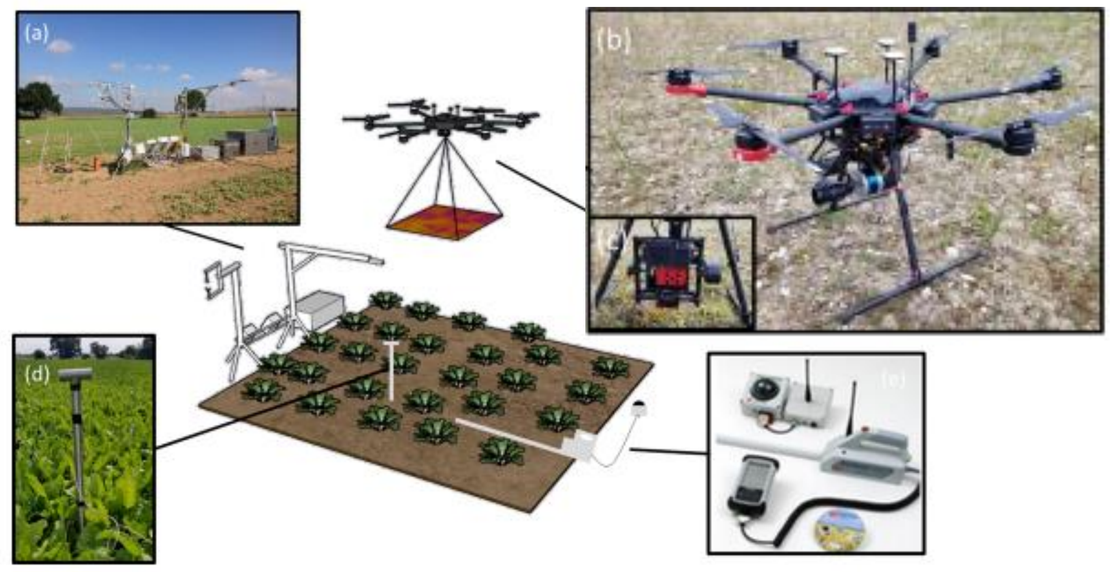

Figure 2. Equipment used in this study with (a) climate station / flux tower located in the center of the field for model inputs and validation of ET estimations (b) DJI Matrice 600 multirotor UAS with LiDAR for crop height (c) thermal IR and multispectral sensors used for land surface temperature and leaf area index (d) measuring stick for crop height validations (e) SunScan SS1 comptometer for LAI calibrations and validations

Methods

TSEB-PT Model

The two-source energy balance model developed by Normal et al. (1995), partitions soil and vegetation components.

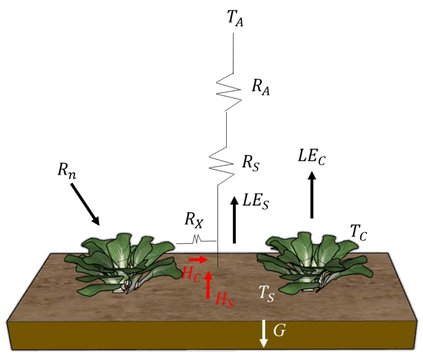

Figure 3. Schematic representation of TSEB with $\mathbf{T_A}$: Air Temperature, $\mathbf{R_A}$: aerodynamic resistance (soil/canopy system), $\mathbf{R_S}$: aerodynamic resistance (boundary layer), $\mathbf{R_X}$:boundary layer resistance of canopy leaves, $\mathbf{T_{AC}}$: temperature of canopy – air space, $\mathbf{T_C}$: canopy temperature, $\mathbf{T_S}$: soil temperature, $\mathbf{LE_S}$: latern heat flux (soil), $\mathbf{LE_c}$: latent heat flux (canopy), $\mathbf{H_S}$: sensible heat flux (soil), $\mathbf{H_c}$: sensible heat flux (canopy), $\mathbf{G}$: soil heat flux

In the TSEB model, the surface-energy budgets are balanced for both the soil and canopy components of the scene:

$$R_n = LE + H + G,$$
$$R_{nc} = H_c + LE_c,$$
$$R_{ns} = H_s + LE_s + G,$$

Rn is net radiation (W m−2), H is sensible heat flux (W m−2), LE is latent heat flux (W m−2), and G is soil heat flux (W m−2). Subscripts "s" and "c" represent the soil and canopy flux components, respectively.

Three primary inputs are derived from UAS sensor observations: radiometric surface temperature, the leaf area index (LAI) for leaf distribution, and crop height (surface roughness) to understand the aerodynamic roughness and radiation transmission in crops and calculate foliage density.

Land surface temperature from UAS Thermal IR

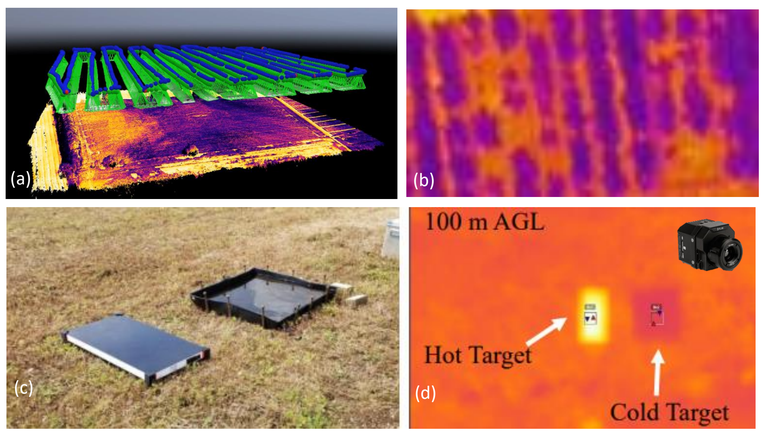

Figure 4. (a) flight path of UAS with land surface temperature mosaic below (b) approximately 11 cm ground sampling distance (GSD) at 100m flight altitude (c) ground targets for thermal sensor for examining and improving (d) ground targets as seen by the thermal IR sensor

Crop Height from UAS LiDAR

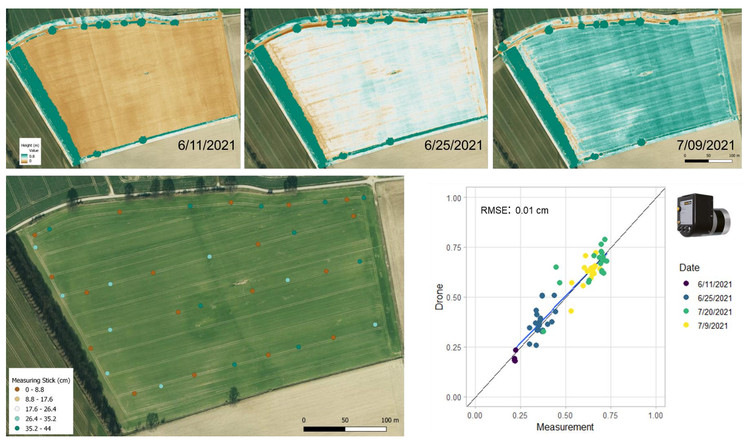

Figure 5. UAS LiDAR derived crop height compared with with measuring stick samples evenly distributed across the field

LAI from UAS Multispectral

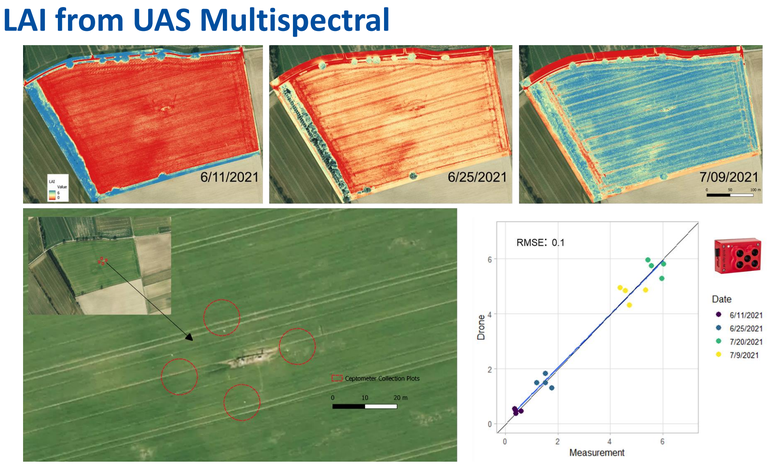

Figure 6. UAS LiDAR derived leaf area index (LAI) compared with Sunscan SS1 ceptometer measurements taken around the climate station in the middle of the field. An average was taken from 15 measurements in each of the 4 locations.

UAS ET Estimation Validation

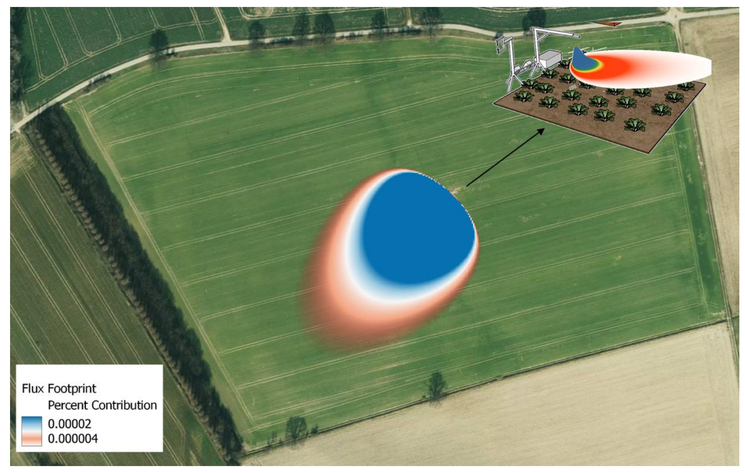

Figure 7. The results of the TSEB model are evaluated in comparison to estimations made with a flux tower and eddy-covariance (EC) from the climate station. The flux footprints were estimated where the weighted average within this boundary of the UAS data was extracted and compared to the EC results.

Results

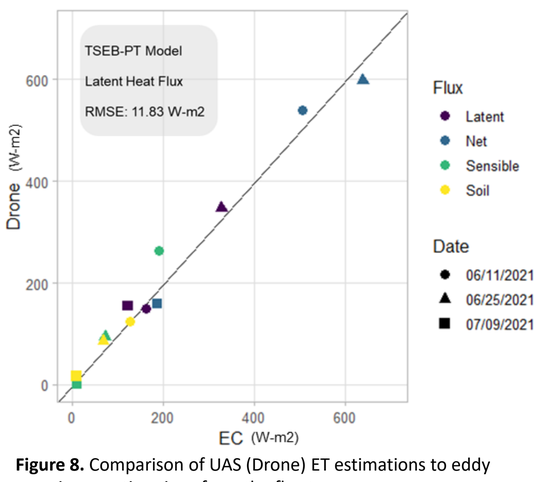

Figure 8. Comparison of UAS (Drone) ET estimations to eddy covariance estimations from the flux tower

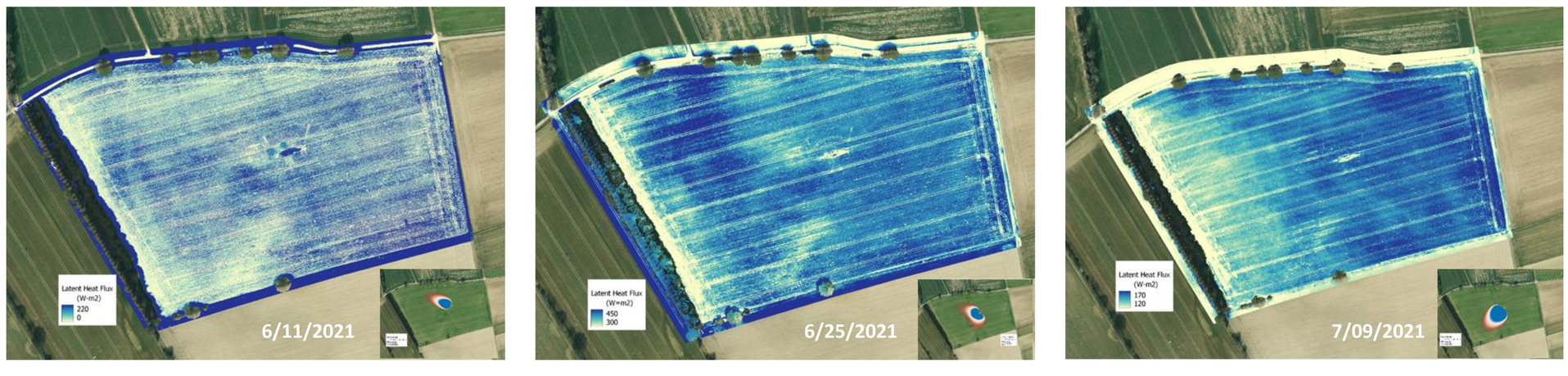

Figure 9. Visualized latent heat flux estimations from TSEB model results and UAS data with the estimated flux foot print that was used to compare the results to the eddy covariance estimations for validation

[1] Norman, J.M.; Kustas, W.P.; Humes, K.S. Source approach for estimating soil and vegetation energy fluxes in observations of directional radiometric surface temperature. Therm. Remote Sens. Energy Water Balance Veg. 1995, 77, 263–293.